Evidence of negative spin polarization in ferromagnetic Sr_2FeMoO_6 as observed in a magnetic Compton profile study

Aniruddha Deb*
Material Science Division, Japan Synchrotron Radiation Research Institute (JASRI/SPring-8), Mikazuki, Sayo, Hyogo 679-5198, Japan and Environmental Energy Technologies Division, Lawrence Berkeley National Laboratory, One Cyclotron Road, Berkeley, California 94720, USA

N. Hiraoka,† M. Itou, and Y. Sakurai
Material Science Division, Japan Synchrotron Radiation Research Institute (JASRI/SPring-8), Mikazuki, Sayo, Hyogo 679-5198, Japan

A. Koizumi
Graduate School of Material Science, University of Hyogo, Kamigori, Ako, Hyogo 679-5198, Japan

Y. Tomioka
Correlated Electron Research Center, National Institute of Advanced Industrial Science and Technology (AIST), Tsukuba, Ibaraki 305-8562, Japan

Y. Tokura
Correlated Electron Research Center, National Institute of Advanced Industrial Science and Technology (AIST), Tsukuba, Ibaraki 305-8562, Japan
and Department of Applied Physics, University of Tokyo, Tokyo 113-8656, Japan
(Received 7 May 2004; revised manuscript received 15 June 2004; published 20 September 2004)

The spin-polarized electron momentum distribution [magnetic Compton profile (MCP)] of ferromagnetic Sr_2FeMoO_6 has been measured, using the magnetic Compton scattering technique, at temperatures 10 K and 300 K, for the [100] and [110] crystallographic directions. The experimental results have been compared with results from electronic structure calculations performed utilizing the full potential linearized augmented plane-wave method. The calculated results clearly show that only down-spin states contribute to the E_F intensity (half metallic character). The experimental observations clearly show evidence for the existence of negative spin polarization that arises from down-spin bands. We have observed the change in the MCP, which arises from the band spin fluctuation, between the low temperature 10 K and high temperature 300 K.

DOI: 10.1103/PhysRevB.70.104411 PACS number(s): 75.25.+z, 78.70.Ck, 71.18.+y, 71.15.Ap

The observation of colossal magnetoresistance (CMR) in the perovskite mixed valent manganites has led to a renewed interest in ferromagnetic oxides. It is believed that the double-exchange mechanism in the presence of strong electron-phonon couplings arising from Jahn-Teller distortions is responsible for the observed properties in the manganites.[1] However, CMR phenomena have been stimulating a significant attention on the research on the manganese oxides because of their potential applications to magnetotransport devices and also due to their interesting physics. For industrial applications, one of the ideal properties is to work in a low magnetic field at room temperature. In this respect tunneling magnetoresistance (TMR) is more attractive than CMR. To realize such properties, the electronic structure should ideally have half-metallic density of states with high Curie temperature. Though some of the manganites are half metallic,[2] many of them have low T_c and need a high magnetic field. Recently, Kobayashi *et al.*[3] reported that ordered Sr_2FeMoO_6 shows a large TMR and also the half-metallic density of states as seen in manganites. Sr_2FeMoO_6, in contrast to manganites, has certain technologically desirable properties, such as a substantial MR at a low applied field even at room temperature. Saitoh *et al.*[4] utilizing photoemission spectroscopy confirmed the origin of the first peak crossing E_F and the second peak well below E_F. While the former is mainly dominated by (Fe+Mo) t_{2g} states the latter is mainly dominated by the Fe e_g states, confirming that the down-spin states contribute to the E_F intensity. From the fundamental point of view, it is important to note that the crystallographic data indicate no substantial Jahn-Teller (JT) distortion and, therefore, the lattice appears to play a less significant role in this compound. Furthermore, the system is an undoped one in contrast to the manganites. Hence this compound is in principle a much simpler system to understand, regarding its properties in detailed theoretical terms. In spite of this apparent simplicity, there have been various conflicting issues concerning its magnetic and electronic structures.

The structure of Sr_2FeMoO_6 is built of perovskite blocks where the transition metal sites are alternatively occupied by Fe and Mo ions. In this compound it is believed that the $Fe^{3+}(3d^5, S=5/2)$ ion is antiferromagnetically coupled to their six $Mo^{5+}(4d^1, S=1/2)$ nearest neighbors, leading to a total saturation magnetization $M_S=4\ \mu B/f.u.$ An alternative picture has also been suggested where the system shows the same M_S value, assigned $Fe^{2+}(3d^6, S=2)$ and $Mo^{6+}(4d^0)$, and a ferromagnetic superexchange coupling between the Fe^{2+}

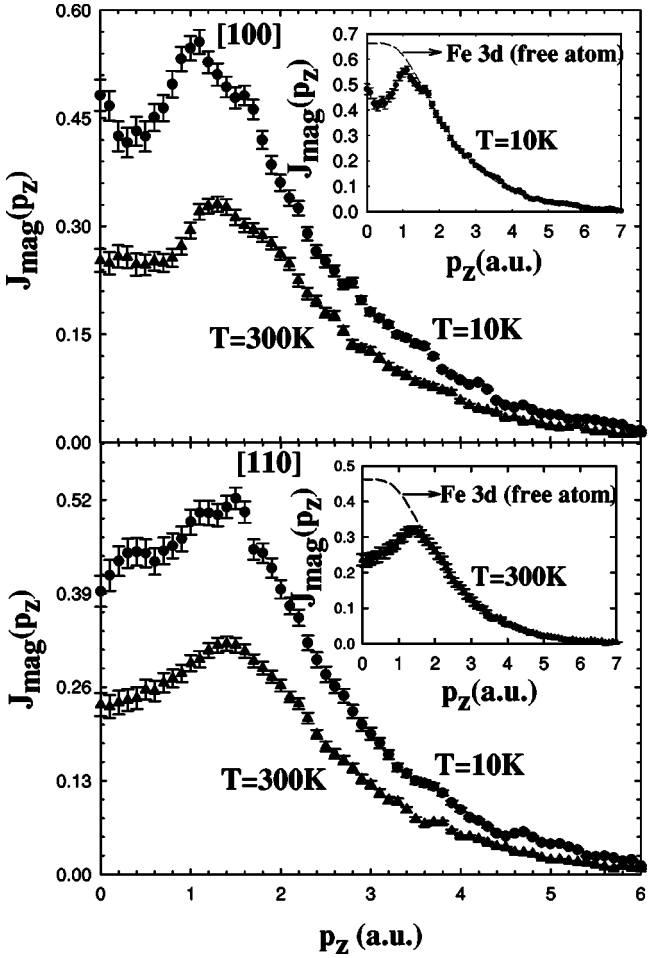

FIG. 1. The experimental magnetic Compton profile of Sr_2FeMoO_6 measured at 10 K (solid circles) and 300 K (solid triangles) along the [100] and [110] crystallographic directions. The inset shows the comparison between the HF free atom fit (dashed lines) and the observed MCP at 10 K (solid circles) (upper panel) and at 300 K (solid triangles) (lower panel).

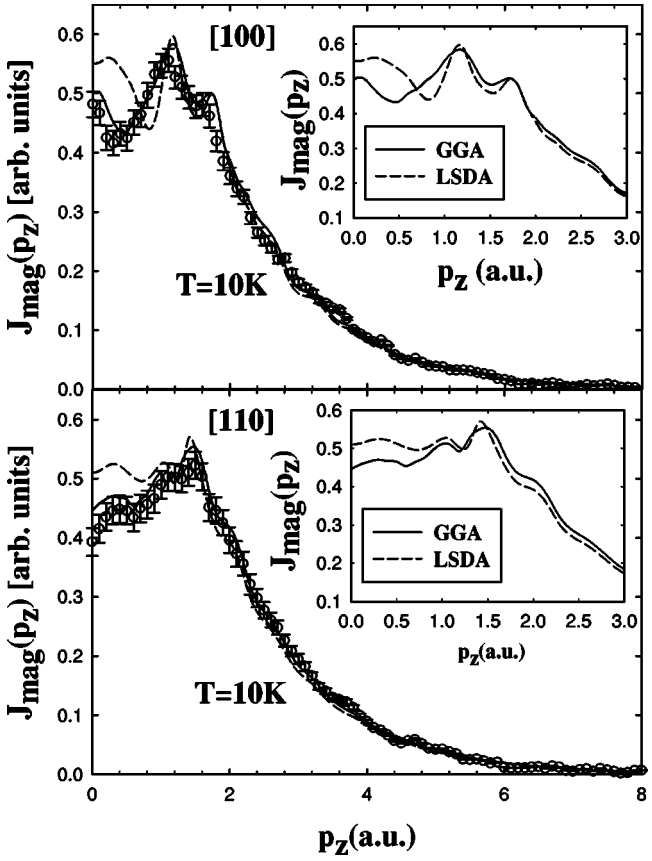

FIG. 2. The experimental MCP at 10 K (circles), calculated FLAPW (GGA) (solid line), and calculated FLAPW (LSDA) (dashed lines) along the [100] and [110] crystallographic directions. The inset shows the comparison of the FLAPW-LSDA (dashed lines) and the FLAPW-GGA (solid line) results in the low-momentum region (0–3 a.u.). The $J_{mag}(p_z)$ in the inset is in arbitrary units.

ions is assumed. But this picture has only been fairly consistent with the neutron-diffraction results,[5] which reported that $\mu_{Fe}=4.1\ \mu_B$ and μ_{Mo} is indefinable between 0.0 μ_B and 0.42 μ_B. Another neutron-diffraction result[6] suggests $\sim 1\ \mu_B$ magnetic moment at the Mo site. Moreover, Mössbauer results were analyzed both in terms of Fe^{3+} (Ref. 7) and $Fe^{2.5+}$ (Ref. 8) states. Double perovskite ($A_2BB'O_6$) crystallizes in the rocksalt structure with alternate units ABO_3 and $AB'O_3$ along three crystallographical axes. The corners of each perovskite unit are in turn occupied by transition metal atoms B and B' with oxygen atoms located in between, forming alternate BO_6 and $B'O_6$ octahedra. The large alkaline-earth-metal atom A occupies the body-centered site with a 12-fold oxygen coordination in each unit. In the ionic model, the transition-metal ions are in the $(BB')^{8+}$ valence state. The frequently believed ferrimagnetic half-metallic ground state is argued to be unstable because of the competition between the generalized double-exchange mechanism, operating in the hybridized t_{2g} bands of Fe 3*d* and Mo 4*d* orbitals in the metallic minority-spin channel, and the strong antiferromagnetic superexchange interactions in the Fe sublattice, mediated by virtual electron hopping into the unoccupied Mo 4*d* states.[9] Possible mechanisms responsible for a stable magnetic ground state such as spin-spiral ordering, spin canting, breathing distortion, and disorder, as well as antisite defects, were also discussed in Ref. 9. Thus, it is obvious that the basic issues concerning the electronic and magnetic structures of this compound are still being investigated. Since the analyses of the Mössbauer and neutron data are model dependent, it is therefore necessary to obtain a site-specific direct information concerning the electronic and magnetic properties of this compound under consideration and hence motivated us for the present experimental magnetic Compton scattering investigation. With the more direct access of the spin-dependent electron momentum density provided by the magnetic Compton scattering technique, we decided to confront highly accurate full-potential linear augmented plane-wave method utilizing the generalized gradient approximation scheme (FLAPW-GGA) computations with the corresponding experimental measurements.

An energy spectrum of Compton scattered x rays, induced by circularly polarized x rays, provides information about the momentum distribution of the spin-polarized electrons.[10] Within the impulse approximation,[11] the spin-dependent dif-

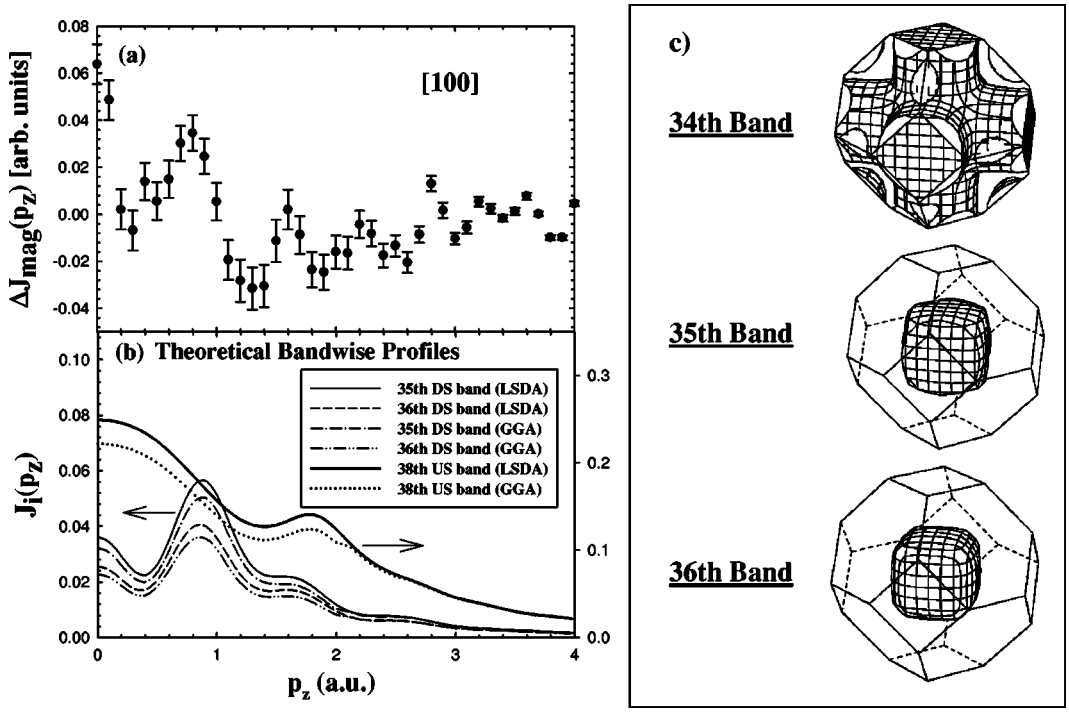

FIG. 3. (a) The difference in the experimental MCP $[\Delta J_{\mathrm{mag}}(p_z)]$ observed at 10 K and 300 K along the [100] crystallographic direction. For details see text. (b) The individual theoretical FLAPW band-wise profile contribution near the Fermi level. The band-wise profiles shown are the down-spin (DS) 35th (GGA, dash-dot line; LSDA, solid line) and 36th bands (GGA, dash-double-dotted line; LSDA, dashed line) and the up-spin (US) 38th band (GGA, dotted line; LSDA, thick solid line) contribution along the [100] crystallographic direction. (c) Shows the Fermi surface nature for the down-spin 34th, 35th, and the 36th bands, respectively.

ferential scattering cross section is proportional to the magnetic Compton profile (MCP), $J_{\mathrm{mag}}(p_z)$, defined as the one-dimensional projection of the spin-polarized electron momentum distribution:

$$\left[\frac{d^2\sigma}{d\Omega d\omega}\right]_{spin} \propto J_{mag}(p_z) = \iint [n_\uparrow(p) - n_\downarrow(p)]dp_x dp_y, \quad (1)$$

where $n_\uparrow(p)$ and $n_\downarrow(p)$ represent the momentum densities of the majority- and minority-spin bands, respectively. The area under the MCP is proportional to the total spin moment (μ_{spin}) per formula unit (FU):

$$\int_{-\infty}^{+\infty} J_{mag}(p_z)dp_z = \mu_{spin}. \quad (2)$$

When the MCP can be decomposed into a few partial profiles with the characteristic shape of a specific electronic state, the area under the partial profile gives the partial spin moment associated with that state. In this paper, we present the MCS study on a well-characterized single crystal of Sr_2FeMoO_6.

Detailed procedures of the sample preparation and characterization were reported earlier by Tomioka *et al.*[12] The single crystals were prepared by the floating-zone method, exhibit a Curie temperature of about 420 K, and the saturation magnetization at 5 K was about 3.2 μ_B per formula unit. This deviation from the ideal value of 4 μ_B was discussed by Tomioka *et al.*[12] The magnetic Compton profiles of Sr_2FeMoO_6 were resolved along the two major crystallographic directions as a function of temperature at the high-energy inelastic scattering beamline BL08W at the SPring-8, Japan. Circularly polarized x rays emitted from an elliptical multipole wiggler were monochromatized to 271 keV and incident on the sample. At these photon energies, which is desirable for optimum resolution and interpretation within the impulse approximation, reversing the helicity of the incident photons is not practical, the spin-dependent signal being here isolated by reversing the sample's magnetization vector utilizing a 3-*T* superconducting magnet. The scattered x rays with a scattering angle of 178.5° were energy analyzed by a ten-element Ge detector. The overall momentum resolution was 0.45 atomic units (a.u., where 1 a.u=1.99 $\times 10^{-24}$ kg m s^{-1}). Since MCP is the difference between two Compton profiles, components arising from spin-paired electrons and from most sources of systematic error are effectively cancelled out. During measurements, the direction of the magnetization in the sample was achieved by an external magnetic field of ±2.5 T applied alternatively along the [100] and [110] crystallographic directions of the sample. The MCP's were extracted as a difference of Compton scattering intensities in reversing the direction of the external field with a fixed photon polarization. Before summing up the magnetic data, they were corrected for energy-dependent detector efficiency, sample absorption, and the relativistic scattering cross section. After checking that the resulting spectra were symmetric about $p_z=0$, the profiles were folded to increase the effective statistics. Finally, the magnetic Compton profiles were normalized to the spin moment per formula unit. The saturation magnetization of the single crystals were measured using a superconducting quantum inter-

ference device (SQUID) magnetometer at 10 K and 300 K, and is assumed to be entirely due to spin contribution and is preferred for the normalization of the data. The saturation moment at 10 K and 300 K were found to be 2.98 μ_B and 1.88 μ_B, respectively.

The spin-dependent electron momentum distributions for Sr_2FeMoO_6 were calculated using the full-potential linearized augmented plane-wave (FLAPW) method. The exchange-correlation part of the potential was described in the GGA.[13] A mesh of 230 inequivalent k points in the irreducible Brillouin zone was used for the k space integration. Compton profiles were calculated along the three major direction [100], [110], and [111] directions. The overall feature of our results is consistent with the calculation done by Kobayashi *et al.*[3] Our calculated results show that the down-spin conduction band crossing E_F is dominated by the Fe $3d-$Mo $4d$ $t_{2g\downarrow}$ states while the O $2p$ states have smaller contribution. On the other hand, the up-spin band just below E_F is mostly ascribed to the Fe $3d$ $e_{g\uparrow}$ and the O $2p$ states without any appreciable Mo $4d$ contribution. As seen from Fig. 1, there is a significant difference in the shape of the MCP's along the [100] and [110] crystallographic directions, between the low-temperature, 10 K, and the high-temperature, 300 K, data. For comparison, a free-atom Hartree-Fock (HF) profile of Fe $3d$ is shown in the inset of Fig. 1. So far, free-atom (HF) wave functions have been successfully used to analyze the data of different systems [14] where magnetic Compton scattering has been used in a site-specific manner. However, the HF wave functions fail to reproduce the low-momentum (p_z) results where solid-state effects are manifested. The one-dimensional projection of the spin moment momentum distribution calculated using FLAPW method for Sr_2FeMoO_6 resolved along the [100] and [110] directions at 10 K is shown in Fig. 2. The calculated MCP is in good agreement with that measured experimentally; high-momentum tails of the experimental profiles (above 7 a.u.) are well matched with the profiles calculated theoretically in that both the experiment and the calculated profiles mutually go to zero as expected. However, as compared to the FLAPW-GGA results, the FLAPW calculated results using the local spin density approximation (LSDA) produce a worse MCP agreement with the experimental results in both crystallographic directions in the momentum region below 3 a.u.; this is shown in the inset of Fig. 2. The observed changes in the profiles along the [100] and [110] directions for the two temperatures (10 K and 300 K) are shown in Figs. 3 and 4, respectively. To compare the temperature-dependent Compton profiles we have normalized the directional data for the two measured temperatures as

$$\Delta J_{mag}(p_z) = J_{mag,10\ K}(p_z) - \alpha * J_{mag,300\ K}(p_z), \qquad (3)$$

where α represents the normalization factor when the two observed profiles at two corresponding temperatures are normalized to the same area for direct comparison. Figures 3(a) and 4(a) show the difference in the MCP between the 10 K and 300 K along the [100] and [110] crystallographic directions. To investigate the difference and shape of the MCP's

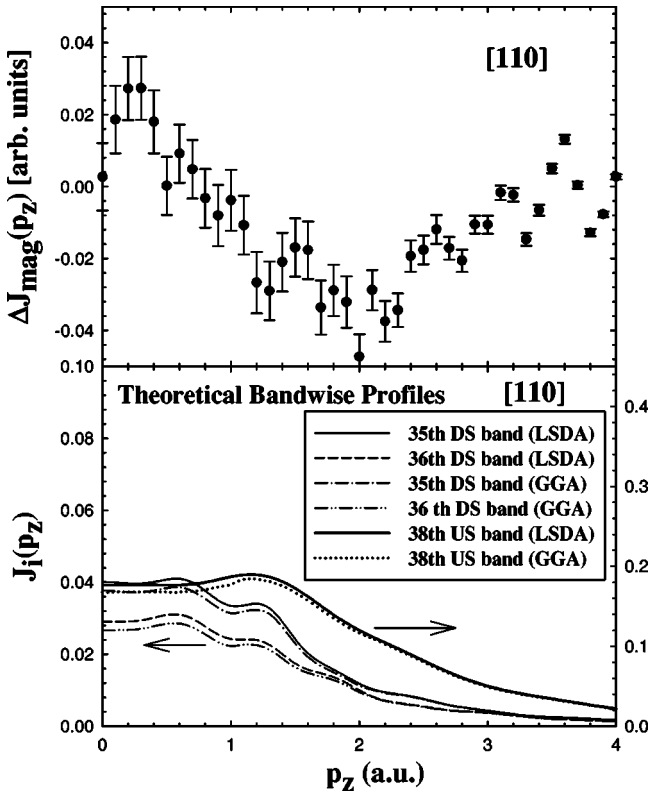

FIG. 4. (a) The difference in the experimental MCP [$\Delta J_{mag}(p_z)$] observed at 10 K and 300 K along the [110] crystallographic direction. For details see text. (b) The individual theoretical FLAPW band-wise profile contribution near the Fermi level. The band-wise profiles shown are the down-spin (DS) 35th (GGA, dash-dotted line; LSDA, solid line) and 36th bands (GGA, dash-double-dotted line; LSDA, dashed line) and the up-spin (US) 38th band (GGA, dotted line; LSDA, thick solid line) contribution along the [110] crystallographic direction.

observed at these two temperatures, we have also calculated the individual band-wise profiles contributing to the MCP's. For this we have shown the major contribution to the MCP's obtained using GGA and LSDA schemes, from the down-spin bands 35th and 36th and the up-spin 38th band contribution in Figs. 3(b) and 4(b), respectively. In the previous literature, there has been no mention or reports of the nature of the Fermi surface of the down-spin individual bands. Here we have shown the nature of the Fermi surface obtained using the FLAPW-GGA calculation (Fig. 3). It is important to note that the nature and shape of the down-spin bands play an important role as the up-spin channel behaves like an insulator with a finite gap at E_F, while the down-spin channel shows a fine density of states (DOS) across the E_F, resulting in a half-metallic character in this perovskite material. The most important consequence of this is that the mobile charge carriers in this system are fully spin polarized. The nature of the Fermi surface for the 34th, 35th, and the 36th down-spin bands is shown in Fig. 3(c). The 34th band forms an electron surface with thick necks along the Γ-X directions, while the 35th and 36th bands form electron surfaces with a nearly rectangular shape. The Fermi surfaces for the 35th and 36th bands have significant flat areas perpendicular to the Γ-X

directions, which predicts a strong Fermi surface nesting.

The contribution to the MCP from 35th and 36th down-spin bands shows a maximum near 1 a.u. in the [100] direction as shown in Fig. 3(b); this is in turn reflected in the difference profile that has been observed between the 10 K and 300 K data where a similar maximum is observed near about 1 a.u. Such an observation can also be noted when we consider the band-wise contribution of the 35th and 36th down-spin band and the 38th up-spin band contribution for the [110] direction. In the down-spin bands, the DOS around the Fermi level originates from the Mo 4*d* t_{2g} and Fe 3*d* t_{2g} electrons, which are strongly hybridized with the O 2*p* states. The fine structures revealed in $\Delta J_{\mathrm{mag}}(p_z)$ indicate the temperature dependence of the nature of the t_{2g} states—e.g., orbital ordering or growth of their Fermi surface bodies. Thus from Figs. 3 and 4 it is now clearly evident that there is the existence of negative spin polarization in this double perovskite system which is arising from the down-spin bands.

In the conclusion, magnetic Compton scattering experiments were performed on the Sr_2FeMoO_6 double-perovskite system. The results were analyzed by self-consistent band structure calculations using the FLAPW-GGA method. Experimental and theoretical investigations of this interesting double perovskite reveal that the FLAPW-GGA calculations provide better agreement especially in the low-momentum region than the FLAPW-LSDA results. The calculations demonstrate that the DOS around the Fermi level originates from the down-spin bands of (Fe+Mo) t_{2g}, consistent with the earlier band structure calculations. Furthermore, the band-wise Compton profile results show that 35th and 36th down-spin bands have Mo and Fe t_{2g} contributions. The experimental results demonstrate evidence for the existence of negative spin polarization which arises from the down-spin bands. The study also reveals that difference in the MCP between the 10 K and the 300 K arises from the band dependent spin fluctuation.

We acknowledge support by the SPring-8 Joint Research Promotion Scheme under the auspices of Japan Science and Technology Corporation. The experiment was performed under the approval of Japan Synchrotron Radiation Research Institute (JASRI), SPring-8 Proposal No. 2002A0564-ND3-np.

*Corresponding author. FAX: (510)486-7303. Electronic address: ADeb@lbl.gov (Aniruddha Deb)

†Present address: ESRF, BP 220, F-38043 Grenoble Cedex, France.

[1] P. W. Anderson, Phys. Rev. **100**, 675 (1955).

[2] J. H. Park, E. Vescovo, H. -J. Kim, C. Kwon, R. Ramesh, and T. Venkatesan, Nature (London) **392**, 794 (1998).

[3] K. I. Kobayashi, T. Kimura, H. Sawada, K. Terakura, and Y. Tokura, Nature (London) **395**, 677 (1998).

[4] T. Saitoh, M. Nakatake, A. Kakizaki, H. Nakajima, O. Morimoto, Sh. Xu, Y. Morimoto, N. Hamada, and Y. Aiura, Phys. Rev. B **66**, 035112 (2002).

[5] C. Ritter, M. R. Ibarra, L. Morellon, J. Blasco, J. Garcia, and J. De Teresa, J. Phys.: Condens. Matter **12**, 8295 (2000).

[6] Y. Moritomo, Sheng Xu, Akihiko Machida, Takumi Akimoto, Eiji Nishibori, Masaki Takata, Makoto Sakata, and Kenji Ohoyama, J. Phys. Soc. Jpn. **69**, 1723 (2000).

[7] T. Nakagawa, K. Yoshikawa, and S. Nomura, J. Phys. Soc. Jpn. **27**, 880 (1969).

[8] J. Linden, T. Yamamoto, M. Karppinen, H. Yamauchi, and T. Pietari, Appl. Phys. Lett. **76**, 2925 (2000).

[9] I. V. Solovyev, Phys. Rev. B **65**, 144446 (2002).

[10] N. Sakai, J. Appl. Crystallogr. **29**, 81 (1996).

[11] P. Eisenberger and P. M. Platzman, Phys. Rev. A **2**, 415 (1970).

[12] Y. Tomioka, T. Okuda, Y. Okimoto, R. Kumai, K.-I. Kobayashi, and Y. Tokura, Phys. Rev. B **61**, 422 (2000).

[13] J. P. Perdew, K. Burke, and M. Ernzerhof, Phys. Rev. Lett. **77**, 3865 (1996).

[14] J. T. Okada, Y. Watanabe, Y. Yokoyama, N. Hiraoka, M. Itou, Y. Sakurai, and S. Nanao, J. Phys.: Condens. Matter **14**, L43 (2002).